Published in final edited form as:
NMR Biomed. 2011 July ; 24(6): 561–568. doi:10.1002/nbm.1590.

Molecular imaging of tumor invasion and metastases: the role of MRI†

Thomas E. McCann[a], **Nobuyuki Kosaka**[a], **Baris Turkbey**[a], **Makoto Mitsunaga**[a], **Peter L. Choyke**[a], and **Hisataka Kobayashi**[a,*]

[a]T. E. McCann, N. Kosaka, B. Turkbey, M. Mitsunaga, P. L. Choyke, H. Kobayashi Molecular Imaging Program, Center for Cancer Research, National Cancer Institute, National Institutes of Health, Bethesda, MD, USA

Abstract

The processes of tumor invasion and metastasis have been well characterized at the molecular level, and numerous biomarkers of tumor aggressiveness have been discovered. Molecular imaging offers the opportunity to depict specific cell markers relevant to tumor aggressiveness. Here, we describe the role of MRI in identifying tumor invasiveness and metastasis with reference to other methods. Target-specific molecular imaging probes for tumor invasiveness have been developed for positron emission tomography and optical imaging, but progress in MRI has been slower. For example, proteases associated with tumor invasion, such as specific matrix metalloproteinases or cathepsins, can be targeted *in vivo* using optical and positron emission tomography methods, but have not yet been successful with MRI. In addition, we describe the use of MRI to detect metastases. Novel MR contrast agents based on iron oxide and dendrimer nanomaterials allow for better characterization of tumor metastases. Organ-specific MR contrast agents are used to identify metastatic disease in the liver. Finally, diffusion-weighted whole-body MRI is discussed as an alternative offered by MRI that does not require the use of molecular probes to screen distant metastases.

Keywords

cancer; invasion; metastasis; molecular imaging; MRI; PET; optical imaging

INTRODUCTION

The progression of cancer from a single tumor nodule to metastatic disease occurs at different rates for different tumors (1). Although the rate of progression may differ among tumors, it is thought that the majority of tumors undergo a series of steps that lead to the expression of an invasive phenotype prior to metastasis. Many of these steps have been characterized at the molecular level *in vitro*; however, the visualization of these phenotypes *in vivo* remains elusive.

Molecular imaging represents a broad range of new technologies that incorporate advances in imaging sciences with progress in molecular biology. Molecular imaging has been defined as the *in vivo* characterization and measurement of biological processes at the cellular and molecular level (2). The ultimate goal of developing molecular imaging is to

*Correspondence to: H. Kobayashi, Molecular Imaging Program, Center for Cancer Research, National Cancer Institute, National Institutes of Health, Building 10, Room B3B69, MSC1088, Bethesda, MD 20892-1088, USA..

identify tumor-specific biomarkers that enable the `personalization' of cancer therapy, depending on the characteristics of each patient's individual cancer. Personalized therapy should lead to better long-term outcomes with less morbidity.

Advances in molecular imaging have led to the development of novel imaging probes that can be used with current imaging modalities to identify cell-specific targets *in vivo*. Imaging probes that can identify the steps leading to metastasis could serve as molecular markers of disease status. Such probes could be used to estimate invasiveness and guide therapy in patients. However, techniques such as positron emission tomography (PET) and optical imaging have a natural advantage over MRI because their sensitivity is several orders of magnitude greater; thus, early work has focused on these modalities. Slowly, progress is being made in molecular imaging with MRI.

An important determinant of patient treatment is the presence or absence of metastases. The establishment of tumor metastases represents the terminal step of most cancers. The development of novel agents to aid in the accurate diagnosis of early metastatic disease would prove important in patient staging and would allow for the early initiation of therapy.

In this article, as the MRI probe is not useful for detecting tumor invasiveness, we describe advances in PET and optical imaging for the detection of tumor invasiveness using probes to visualize matrix metalloproteinases (MMPs) and cathepsin activity. Next, we review current MR contrast agents with reference to their ability to detect metastases. Finally, we discuss how advances in technology, such as the development of diffusion-weighted (DW) MR in the context of whole-body (WB) imaging, can be helpful in the assessment of metastases, and may act as an alternative to `probe based' molecular imaging.

MOLECULAR IMAGING PROBES TO CHARACTERIZE TUMOR INVASIVENESS

Invasiveness is the characteristic of a tumor, whereby it is no longer contained at the tumor-host interface and has the capability to spread unpredictably through tissue. The molecular events that lead to a progressively more invasive phenotype are numerous. One characteristic of tumor aggressiveness is the ability to recruit stromal and lymphatic cells to develop a microenvironment that facilitates tumor progression; however, such features are not unique to invasive tumors. For instance, tumor-associated macrophages are involved in tumor cell migration, invasion and metastasis, but can also be found in tumors that have not yet progressed (3). Macrophages interact closely with tumor cells, the extracellular matrix (ECM) and blood vessels.

In order for the tumor to extend its borders, enzymatic activity is required. Among the enzymes implicated in tumor invasiveness, MMPs are a family of differentially expressed proteases that rearrange and degrade components of the ECM to aid in tumor invasion (4). There are over 20 known MMPs, and tight spatial and temporal regulation give MMPs detailed roles in the process of invasion and metastasis (4). Such fine-tuning and differential expression provide a target for the therapeutic inhibition of specific MMPs. Other proteases have also been reported to play a role in invasion. For example, cathepsin, a member of the papain subfamily of cysteine proteases, has also been implicated in tumor invasiveness (5). Normally, cathepsins are expressed and remain intracellular; however, as cells gain invasive potential, cathepsins are secreted into the extracellular environment where they play a role in ECM remodeling (5).

Currently, there is no wholly satisfactory imaging method for the visualization of tumor invasiveness in clinical practice. Although MRI has proven itself as an anatomic method for

detecting tumor invasiveness at a macroscopic level, it has not yet been harnessed to provide information at the molecular level. However, a number of other imaging techniques have been developed that have had some success in visualizing the invasive phenotype. These techniques, and their success in early clinical trials, have been reviewed elsewhere (6). As MRI does not play a major role in this arena, we describe the use of targeted PET and optical imaging probes to identify proteases associated with biological tumor invasiveness.

A specific member of the MMP family, MMP-2, is associated with the invasiveness of breast, lung, gastric and esophageal cancers (4). MMPs are inhibited *in vivo* by endogenous tissue inhibitors of MMPs (TIMPs). These endogenous inhibitors and the ligands used to bind MMPs have led to the development of numerous MMP-targeted imaging probes using a variety of radioisotopes (7–10). TIMPs are attractive as potential MMP-specific probes not only because they target MMPs, but also because they inhibit MMP activity and thus may also have therapeutic potential. By employing PET, Furumoto et al. (11) synthesized the MMP-2-specific inhibitor, (2R)-2-[4-(6-[^{18}F]fluorohex-1-ynyl)-benzenesulfonylamino]-3-methylbutyric acid ([^{18}F]SAV03) and its prodrug ([^{18}F]SAV03M), and analyzed both agents as potential PET imaging probes. Both [^{18}F]SAV03 and its prodrug demonstrated tumor-specific uptake in a mouse tumor model. However, [^{18}F]SAV03 demonstrated high liver and small intestine uptake, suggestive of rapid breakdown via first-pass metabolism. [^{18}F]SAV03M demonstrated lower liver uptake and higher tumor uptake, leading to the conclusion that it is superior to [^{18}F]SAV03 as a PET agent (11). This demonstrates how the metabolism and biodistribution of PET probes play an important role in the development of PET agents. In addition, the authors were unable to conclude whether the measured uptake signal represented the expression or enzymatic activity of MMP-2.

TIMP2, a specific inhibitor of MMP-2, has also been used to identify MMP-2 activity *in vivo*. Kulasegaram *et al.* (12) synthesized ^{111}In-DTPA-N-TIMP2 (DTPA, diethylenetriaminepentaacetic acid) to be used as a PET agent in human immunodeficiency virus-positive patients with Kaposi's sarcoma (KS). *In vitro* studies revealed that MMP inhibitors could prevent early vascular invasion of KS cells. However, despite its favorable biodistribution, ^{111}In-DTPA-N-TIMP2 was unable to identify KS tumors in humans.

Using fluorescence imaging technology, Jiang (13) employed MMP enzymatic expression to induce tumor cellular uptake of a fluorophore. Polycationic polyarginine-based cell-penetrating peptides (CPPs) were used. CPPs exhibit cellular uptake after electrostatic attachment of the polycationic domain to negatively charged phospholipids and glycosaminoglycans on cell surfaces. Cellular uptake of CPPs can be blocked by linking an inhibitory polyanionic domain to CPPs. By including an enzyme-specific cleavage sequence in the linker between the polycationic and polyanionic domains, and by attaching a near-infrared (NIR) fluorophore to the polycationic domain, enzyme-activated deliverable CPPs were created. These enzyme-activated deliverable CPPs are able to use CPPs to shuttle fluorophores into cells, but this can only occur after enzymatic cleavage of the linker to release the inhibitory domain. This was used to demonstrate the labeling of human squamous cell carcinoma xenografts *in vivo* in a mouse model (13). The probe was specifically activated in the presence of MMP-2 and MMP-9. Recently, these enzyme-activated deliverable CPPs have undergone methods to better characterize their target specificity, toxicity and pharmacokinetics (14,15). One limitation to the use of enzyme-activated deliverable CPPs is that sufficient time must elapse after the administration of CPPs for unbound CPPs to be removed from the body.

Optical imaging is unique because it permits the identification of enzymatic activity through the use of targeted enzyme-activatable signaling probes. These are probes that have little or no baseline fluorescence emission in the nonactivated state but, when they come into contact

with the appropriate enzyme, they are specifically turned on. The development of protease-specific optical imaging probes has been reviewed recently (16,17). Fluorophores can be synthesized in such a way that they are kept in close proximity to each other by a linker, so that shared electron energy occurs that prevents each fluorophore from emitting light – a process known as Forster resonance energy transfer. The linker can be made to contain an enzyme-specific cleavable peptide sequence. When the probe interacts with the target enzyme, the linker is cleaved. This allows the separation of the fluorophores so that they can emit light normally.

This was demonstrated using NIR fluorophores combined with protease-specific `smart probes' to create activatable molecular imaging probes. The use of a NIR fluorophore has the advantage of added tissue depth penetration as a result of decreased absorption and scatter of light at NIR wavelengths. In WB *in vivo* imaging, NIR probes are less influenced by autofluorescence than are green fluorophores which are excited by the same wavelengths that excite autofluorophores. Activatable smart probes were introduced by Tung *et al.* (18,19), who synthesized an activatable NIR probe specific to cleavage by the protease, cathepsin D. Tung *et al.* used a long-circulating poly-L-lysine/methoxypolyethylene glycol graft copolymer (protected graft copolymer, PGC), which has been shown to accumulate in tumors by pinocytosis, as a vehicle. They synthesized a cathepsin D-specific cleavable peptide sequence and conjugated it to the PGC molecule. Cyanine 5 was then attached to the N-terminus of the synthetic peptide. The final probe demonstrated little fluorescent signal at baseline but, in the presence of tumor xenografts that overexpressed cathepsin D, a robust fluorescent signal was appreciated (Fig. 1). This was the first study to demonstrate the use of fluorescent optical imaging probes to visualize protease activity *in vivo*.

Thus, significant advances have been made in imaging the enzymes specifically associated with tumor invasiveness. The low concentration of these enzymes in the peritumoral environment currently demands the use of high-sensitivity PET and optical imaging to detect the target over the background signal. Although attempts have been made to create activatable MR contrast agents that are enzyme based, to date there has been limited success in demonstrating the enzymes associated with tumor invasiveness (20).

MRI TO DETECT EARLY CANCER METASTASIS

The development of cancer metastasis profoundly affects patient survival. Therefore, many imaging methods have been developed to depict metastases at an early time point, when intervention is most successful. Among the imaging modalities, MRI stands out as a potential tool for the visualization of local, organ and systemic metastases in the body using different agents and imaging sequences. MRI possesses the benefits of good anatomic detail, excellent soft tissue resolution and no exposure to ionizing radiation. We begin this section by describing the MR contrast agents that have shown promise in the identification of early metastasis, and we conclude with a discussion of the use of WB DW MRI, without contrast agents, to survey metastasis.

New MRI contrast agents

Iron oxide nanoparticles—Superparamagnetic iron oxide (SPIO) nanoparticles are rapidly taken up by macrophages of the reticuloendothelial system (RES). The intracellular localization of SPIO particles serves to create negative contrast on MRI (21,22). Therefore, in organs such as the liver and spleen, where RES cells predominate, SPIO nanoparticles cause a decrease in T_2^* signal intensity. This can be utilized in the assessment of tumors. As metastatic tumors are deficient in macrophages from RES, their uptake of nanoparticles is diminished. Therefore, lesions of the liver and spleen that contain tumor can be identified by areas that are brighter than the surrounding tissue on both T_2 and T_2^*-weighted images.

These cancerous lesions can be distinguished from benign lesions that are bright on T_2*-weighted images, but have decreased signal intensity on T_2*-weighted images.

Detailed investigation of the kinetics of iron oxide nanoparticles has led to the determination that particle size and surface chemical structures dramatically alter the blood half-life and biodistribution of iron oxide nanoparticles (23). Ultrasmall superparamagnetic iron oxide (USPIO) nanoparticles are taken up less avidly by RES cells of the liver and spleen, resulting in a longer plasma half-life (21). Also, by adding molecules to the surfaces of SPIO nanoparticles, such as a dense packing of dextrans, SPIO nanoparticles are stabilized, preventing aggregation and uptake by the liver and spleen, and resulting in a longer plasma half-life.

SPIO nanoparticles are generally categorized by size. Standard-sized SPIO particles range from 60 to 150 nm, have a short half-life (~ 10 min) and can be used to accurately image RES in the liver and spleen. USPIO nanoparticles (10–40 nm) have a longer half-life (~ 90 min) and are used for angiography and to specifically label lymph nodes. Currently, there are several SPIO nanoparticles available commercially. SPIOs include Ferridex (also known as Ferumoxide, AMI-25 or Endorem) (24–26). The USPIOs available include Ferumoxtran-10 [also known as Combidex, AMI 227 or BMS180549 (Advanced Magnetics, Cambridge, MA, USA) and Sinerum (Guerbet, Gorinchem, the Netherlands)] (27,28). However, clinical use in the USA has been hampered by a lack of regulatory approval and commercial availability.

Dendrimers—Dendrimers are a group of highly branched, spherical polymers that can be synthesized with great structural control, and contain an abundance of surface functional groups that serve as a platform for the attachment and presentation of cell-specific targeting groups, solubility modifiers and imaging agents. Each dendrimer consists of a core concentrically surrounded by annular shells, called generations (referred to as G1, G2, G3, etc.), of covalently linked branched interiors (29). These shells can serve as carriers for small chemicals or drugs, effectively forming nanocapsules. The resultant layered structure enables a great deal of control over the size of the dendrimer, which is dependent on the generation number (30). Several types of dendrimer with different cores and interiors are available, including amine, ethylenediamine and diaminobutyl (DAB) cores, and polyamidoamine (PAMAM) and polypropylimine (PPI) interiors. The *in vivo* characteristics of dendrimers are determined by the size of the dendrimer. Kobayashi and Brechbiel (31) demonstrated that changes in the diameter of dendrimer-based MR contrast agents can greatly impact their pharmacokinetics, permeability across the vascular wall, excretion route and recognition by RES.

Lymphatic metastasis

Lymphatic metastases arising from tumor cells are of particular interest because the lymphatic spread of tumor cells generally follows an orderly progression from primary tumor to local lymphatic vessels, where they travel to the first or `sentinel' lymph node (SLN), whereupon they spread to echelon lymph nodes. The premise of sentinel node imaging is that echelon lymph nodes are unlikely to be affected if SLN is normal (32). The presence of metastatic tumor in lymph nodes serves as an important prognostic factor in most cancer types, and is a major criterion for determining the need for adjuvant chemotherapy (33). Thus, reliable identification of SLN is of clinical importance, and a method to accurately characterize lymph nodes as positive or negative for metastatic disease would greatly influence patient treatment strategies.

USPIO particles—Weissleder *et al.* (22) demonstrated the potential of using USPIO nanoparticles as a contrast agent, when they reported that experimental metastatic lymph nodes do not take up USPIO particles. This observation was the first to suggest the use of USPIO particles as contrast agents to detect lymph node metastasis.

Current diagnostic standards in the characterization of lymph nodes involve assessment based on the size of the lymph node, but this incorrectly identifies enlarged benign lymph nodes and misses micrometastases in normal-sized lymph nodes. USPIO nanoparticles provide detailed information regarding the environment within lymph nodes, which may lead to a more accurate distinction between malignant and benign lymph nodes. Also, USPIO nanoparticles can be administered via the injection of an intravenous bolus, enabling the visualization of lymph nodes throughout the entire body with a single injection. This provides an advantage to traditional lymphography, which only images lymph nodes along a specific drainage tract after interstitial injection (34). Lymph node labeling with USPIO nanoparticles has been shown to specifically detect lymph node metastasis in prostate, testicular and renal cancers (35–37).

PAMAM dendrimer-based contrast agents—Dendrimer-based MRI contrast agents have been employed to visualize functional lymphatic drainage with magnetic resonance lymphangiography (MRL). Kobayashi *et al.* (38) used interstitially injected G6 PAMAM dendrimers loaded with gadolinium (Gd) to image systemic and local draining lymphatic ducts and SLNs of mice with breast tumor xenografts using micro-MRL. They found that Gd-G6 dendrimers provided superior temporal and spatial resolution of draining lymphatic ducts and SLNs when compared with the conventional MR contrast agent, Gd-[DTPA]-dimeglumine (39). The same group then used this micro-MRL technique and Gd-G6 dendrimers to accurately distinguish intralymphatic from extralymphatic metastases in mouse lymphoma and carcinoma models (Fig. 2) (40).

Liver metastasis

SPIO particles—SPIO particles have been approved for use as a negative contrast agent for the normal liver parenchyma to visualize benign and malignant hepatic tumors in clinical practice (41). Clinically, SPIO nanoparticle-enhanced MRI has been shown to increase the accuracy of diagnosis of hepatic and splenic malignancies (26,41). SPIO (AMI-25)-enhanced MRI was compared with gadolinium-enhanced MRI in the differential diagnosis of liver tumors. A difference was found using AMI-25 in the distinction between benign and malignant lesions, with AMI-25 being 93% specific *vs* 81.5% for gadolinium-enhanced MRI (24).

PPI dendrimer-based contrast agents—PPI/DAB dendrimers have a pure aliphatic polyamine interior, in contrast with PAMAM dendrimers, which have a large number of amide bonds and short hydrocarbons in the interior component. Based on the principle that less hydrophilic macromolecular agents target the liver, DAB-Am64-(1B4M-Gd)$_{64}$ (PPI/DABG5), containing a PPI/DABG5 dendrimer with a core unit of 64 surface amines, was synthesized and evaluated as a positive liver MR contrast agent (42). PPI/DABG5 homogeneously enhanced the liver parenchyma and was excreted more rapidly through both the liver and kidney than the analogous PAMAM dendrimer of similar molecular size (42). Using PPI/DABG5, the same group was able to visualize metastatic lesions on the liver from colon cancer cells (LS174T) as small as 0.3 mm in diameter in living mice via a reverse contrast image (Fig. 3). The metastatic tumor cells appeared as a dark area, and normal liver tissue, enhanced by DABG5, was bright (42).

Gadolinium ethoxybenzyl diethylenetriaminepentaacetic acid (Gd-EOB-DTPA)—Gd-EOB-DTPA has been developed as a liver-specific contrast agent by a small modification of conventional Gd chelates. Gd-EOB-DTPA gains its liver-specific properties from the lipophilic EOB moiety, which is taken up by hepatocytes through the organic anion-transporting polypeptide. After intravenous injection with Gd-EOB-DTPA, there is initially little difference between Gd-EOB-DTPA and the nonspecific, extracellular Gd-DTPA. However, as Gd-EOB-DTPA is taken up by hepatocytes, the normal liver parenchyma can be visualized by increased T_1 intensity. This liver-specific enhancement can be detected as early as 20 min after injection. This creates a positive contrast enhancement, where normal liver parenchyma is bright on delayed-phase T_1-weighted images. However, metastases to the liver are observed as focal areas of hypointensity relative to the rest of the normal liver parenchyma. Vogl *et al.* (43) demonstrated an improved detection rate of liver metastases, hepatocellular carcinoma and hemangiomas using Gd-EOB-DTPA compared with unenhanced and Gd-DTPA-enhanced images.

DW MRI

Unlike other imaging methods, MRI has the ability to provide insights into the molecular features of a tumor with intrinsic techniques that do not require extrinsic contrast agents. For instance, DW MRI may serve as an effective method to assess the disorganized characteristics of tumors. DWI uses changes in the diffusion of water to provide information about the functional status of cells in tissue. DWI quantifies the Brownian motion of water using a parameter called the apparent diffusion coefficient (ADC). A low ADC is indicative of a restricted Brownian motion of water, and a high ADC indicates a free Brownian motion of water. ADC values are affected by the proliferation of cells. As cells proliferate, they crowd a given area and hinder the diffusion of water, resulting in a lower ADC value. These concepts can be applied to the imaging of tumors to identify metastases. Studies that have demonstrated differences in ADC between benign and malignant lesions in breast and prostate have been performed (44,45). Malignant lesions were determined to have a lower ADC than benign lesions (Fig. 4). It may be controversial as to whether or not DWI can be categorized as molecular imaging; however, DWI has recently been demonstrated to be an important cancer screening and staging tool by detecting metastasis using MRI; it is comparable with fluorodeoxyglucose-positron emission tomography-computed tomography (FDG-PET-CT) employed in clinical practice, but does not use ionizing radiation or a contrast agent, as shown in the next section. Therefore, we discuss DWI, focusing on WB DW MRI, for the detection of metastases in cancer patients.

WB DW MRI

WB MRI combines excellent tissue contrast, high spatial resolution and detailed morphologic and pathologic information obtained with MRI with the added benefit of a WB screening modality in order to cover all possible sites of metastatic disease. As metastases are often unpredictable in their spread, WB MRI is important and can compete with other WB techniques, such as FDG-PET-CT, but without the ionizing radiation exposure. T_2-weighted or fat-suppressed T_2-weighted pulse sequences (e.g. short TI inversion recovery) have been employed for conventional WB MRI; however, WB DW MRI with a low b value has been used recently for the detection of malignancy and showed highly sensitive and specific detectability, which is relevant to FDG-PET-CT (46). DW WB MRI possesses technical advantages over FDG-PET-CT, e.g. cerebral metastases are particularly difficult to identify in FDG-PET-CT because of a high physiological tracer uptake in normal brain tissue, and studies have identified previously unknown metastases in the brain and extremities in up to 17% of cases (46,47). It has been reported that more than 40% of cases of skeletal metastases occur outside the field of view covered by a routine assessment of the

axial skeleton (48,49). Interestingly, despite its excellent contrast in specific soft tissue and parenchymal organs, especially in the brain, bone marrow and liver, WB MRI employing DWI may prove to be most useful in the detection of metastatic disease.

Schlemmer *et al*. (47) compared WB DW MRI for the detection of distant metastases from a variety of tumors with CT as the standard staging method, and a change of therapy based on WB DW MRI findings alone was reported in six of 63 patients (10%).

A lesion-by-lesion analysis comparing WB DW MRI with FDG-PET-CT, as an alternative screening method for the detection of skeletal metastases, demonstrated significantly higher overall diagnostic accuracy (91% *vs* 78%) for the MR-based method. WB DW MRI showed an overall superior sensitivity (94%), partly because smaller lesions (2–5 mm) could be detected, compared with the sensitivity of FDG-PET-CT (78%), where lesions below 5 mm were difficult to detect. Also, numerous additional skeletal metastases were found in the distal extremities with WB DW MRI (50). In addition, WB MRI has shown superiority to FDG-PET-CT in the detection of liver and bone metastases (46).

Presently, ^{99m}Tc phosphonate-based scintigraphy is the standard method for the systemic screening of skeletal metastases. However, at the early stage of disease, lesions may remain invisible in the absence of an osteoblastic response. Furthermore, the misinterpretation of tracer uptake in healing fractures or degenerative disease may lead to false-positive findings. The diagnostic performance of WB DW MRI compared with bone scintigraphy for the detection of skeletal metastases has revealed a higher specificity and sensitivity in the early detection of skeletal metastases (51,52).

CONCLUSION

Tumor metastasis, the final step in cancer progression, is preceded by numerous molecular events that contribute to the metastatic potential of a tumor. Some of these molecular events have been well documented to play a role in the development of an invasive phenotype. Molecular imaging allows the identification of such molecular events *in vivo*; however, the usefulness of the identification of such events and their clinical impact have yet to be determined.

As discussed, enzymatic peritumoral activity is a probable determinant of invasive behavior. An evaluation of the enzymatic features on tumors using molecular probes will allow a more accurate assessment of MMP expression and activity. Advances in chemistry are needed to allow the development of PET probes with a more favorable biodistribution and metabolism profile. Meanwhile, the development of MRI probes for enzyme detection requires significant improvements in the sensitivity of contrast agents.

Early cancer metastasis can be detected with contrast-enhanced MRI. New contrast agents, such as SPIO nanoparticles, provide information regarding the functional environment within the lymph node. This information can then be used to determine whether or not a given lymph node contains metastatic disease. Dendrimers are versatile molecules that permit the fine-tuning of size, labeling and targeting. The utilization of properties, such as size and hydrophobicity, to influence biodistribution may also prove useful in the future. Finally, not all molecular imaging requires a molecular imaging probe. WB DW MRI has the potential to serve as a single-modality screening tool for the assessment of distant tumor metastases without the need for extrinsic molecular imaging probes.

Future advances in both imaging technology and molecular biology will pave the way for agents that can identify tumor invasiveness and metastasis. Looking forward, a broad range of molecular imaging `tools', each of which may one day be selected to evaluate specific

features of a tumor in humans, are being developed. These tools will enable further personalization of medical therapy, tailoring it to each patient's individual risks and benefits.

Acknowledgments

This research year was made possible through the Clinical Research Training Program, a public–private partnership supported jointly by the National Institutes of Health (NIH) and Pfizer Inc. (via a grant to the Foundation for NIH from Pfizer Inc.). This research was supported by the Intramural Research Program of the Center for Cancer Research, NCI/NIH.

Abbreviations used

ADC	apparent diffusion coefficient
CPP	cell-penetrating peptide
DAB	diaminobutyl
DTPA	diethylenetriaminepentaacetic acid
DW MRI	diffusion-weighted MRI
ECM	extracellular matrix
FDG-PET-CT	fluorodeoxyglucose-positron emission tomography-computed tomography
[^{18}F]SAV03	(2R)-2-[4-(6-[18F]fluorohex-1-ynyl)-benzenesulfonylamino]-3-methylbutyric acid
[^{18}F]SAV03M	prodrug of [18F]SAV03
Gd-EOB-DTPA	gadolinium ethoxybenzyl diethylenetriaminepentaacetic acid
KS	Kaposi's sarcoma
MMP	matrix metalloproteinase
MRL	magnetic resonance lymphangiography
NIR	near-infrared
PAMAM	polyamidoamine
PET	positron emission tomography
PGC	protected graft copolymer
PPI	polypropylimine
RES	reticuloendothelial system
SLN	sentinel lymph node
SPIO	superparamagnetic iron oxide
TIMP	tissue inhibitor of MMPs
USPIO	ultrasmall super-paramagnetic iron oxide
WB MRI	*whole-body MRI*.

REFERENCES

1. Sporn MB. The war on cancer. Lancet. 1996; 347:1377–1381. [PubMed: 8637346]
2. Weissleder R, Mahmood U. Molecular imaging. Radiology. 2001; 219(2):316–333. [PubMed: 11323453]

3. Avraamides CJ, Garmy-Susini B, Varner JA. Integrins in angiogenesis and lymphangiogenesis. Nat. Rev. Cancer. 2008; 8:604–617. [PubMed: 18497750]
4. Deryugina EI, Quigley JP. Matrix metalloproteinases and tumor metastasis. Cancer Met. Rev. 2006; 25:9–34.
5. Mohamed MM, Sloane BF. Cysteine cathepsins: multifunctional enzymes in cancer. Nat. Rev. Cancer. 2006; 6:764–775. [PubMed: 16990854]
6. Josephs D, Spicer J, O'Doherty M. Molecular imaging in clinical trials. Target Oncol. 2009; 4(3): 151–168. [PubMed: 19768637]
7. Giersing BK, Rae MT, CarballidoBrea M, Williamson RA, Blower PJ. Synthesis and characterization of ^{111}In-DTPA-N-TIMP-2: a radiopharmaceutical for imaging matrix metalloproteinase expression. Bioconjug. Chem. 2001; 12(6):964–971. [PubMed: 11716687]
8. Oltenfreiter R, Staelens L, Lejeune A, Dumont F, Frankenne F, Foidart JM, Slegers G. New radioiodinated carboxylic and hydroxamic matrix metalloproteinase inhibitor tracers as potential tumor imaging agents. Nucl. Med. Biol. 2004; 31(4):459–468. [PubMed: 15093816]
9. Kopka K, Breyholz HJ, Wagner S, Law MP, Riemann B, Schroer S, Trub M, Guilbert B, Levkau B, Schober O, Schafers M. Synthesis and preliminary biological evaluation of new radioiodinated MMP inhibitors for imaging MMP activity in vivo. Nucl. Med. Biol. 2004; 31(2):257–267. [PubMed: 15013492]
10. Breyholz HJ, Wagner S, Faust A, Riemann B, Holtke C, Hermann S, Schober O, Schafers M, Kopka K. Radiofluorinated pyrimidine-2,4,6-triones as molecular probes for noninvasive MMP-targeted imaging. ChemMedChem. 2010; 5(5):777–789. [PubMed: 20373323]
11. Furumoto S, Takashima K, Kubota K, Ido T, Iwata R, Fukuda H. Tumor detection using ^{18}F-labeled matrix metalloproteinase-2 inhibitor. Nucl. Med. Biol. 2003; 30:119–125. [PubMed: 12623110]
12. Kulasegaram R, Giersing B, Page CJ, Blower PJ, Williamson RA, Peters BS, O'Doherty MJ. In vivo evaluation of ^{111}In-DTPA-N-TIMP-2 in Kaposi sarcoma associated with HIV infection. Eur. J. Nucl. Med. 2001; 28(6):756–761. [PubMed: 11440037]
13. Jiang T. Tumor imaging by means of proteolytic activation of cell-penetrating peptides. Proc. Natl. Acad. Sci. 2004; 101:17, 867–17, 872.
14. Olson ES, Aguilera TA, Jiang T, Ellies LG, Nguyen QT, Wong EH, Gross LA, Tsien RY. In vivo characterization of activatable cell penetrating peptides for targeting protease activity in cancer. Integr Biol (Camb). 2009; 1(5–6):382–393. [PubMed: 20023745]
15. Aguilera TA, Olson ES, Timmers MM, Jiang T, Tsien RY. Systemic in vivo distribution of activatable cell penetrating peptides is superior to that of cell penetrating peptides. Integr Biol (Camb). 2009; 1(5–6):371–381. [PubMed: 20023744]
16. McIntyre JO, Scherer RL, Matrisian LM. Near-infrared optical proteolytic beacons for in vivo imaging of matrix metalloproteinase activity. Methods Mol. Biol. 2010; 622:279–304. [PubMed: 20135290]
17. McIntyre JO, Matrisian LM. Optical proteolytic beacons for in vivo detection of matrix metalloproteinase activity. Methods Mol. Biol. 2009; 539:155–174. [PubMed: 19377965]
18. Weissleder R, Tung C-H, Mahmood U, Bogdanov A. In vivo imaging of tumors with protease-activated near-infrared fluorescent probes. Nat Biotechnol. 1999; 17:375–378. [PubMed: 10207887]
19. Tung C-H, Mahmood U, Bredow S, Weissleder R. In vivo imaging of proteolytic enzyme activity using a novel molecular reporter. Cancer Res. 2000; 60:4953–4958. [PubMed: 10987312]
20. Schellenberger E, Rudloff F, Warmuth C, Taupitz M, Hamm B, Schnorr J. Protease-specific nanosensors for magnetic resonance imaging. Bioconjug. Chem. 2008; 19(12):2440–2445. [PubMed: 19007261]
21. Weissleder R, Elizondo G, Wittenberg J, Rabito CA, Bengele HH, Josephson L. Ultrasmall superparamagnetic iron oxide: characterization of a new class of contrast agents for MR imaging. Radiology. 1990; 175:489–493. [PubMed: 2326474]
22. Weissleder R, Elizondo G, Wittenberg J, Lee AS, Josephson L, Brady TJ. Ultrasmall superparamagnetic iron oxide: an intravenous contrast agent for assessing lymph nodes with MR imaging. Radiology. 1990; 175:494–498. [PubMed: 2326475]

23. Hu FQ, Wei L, Zhou Z, Ran YL, Li Z, Gao MY. Preparation of biocompatible magnetite nanocrystals for in vivo magnetic resonance detection of cancer. Adv. Mater. 2006; 18:2553–2556.
24. Vogl TJ, Hammerstingl R, Schwarz W, Kümmel S, Müller PK, Balzer T, Lauten MJ, Balzer JO, Mack MG, Schimpfky C, Schrem H, Bechstein WO, Neuhaus P, Felix R. Magnetic resonance imaging of focal liver lesions. Comparison of the superparamagnetic iron oxide resovist versus gadolinium-DTPA in the same patient. Invest. Radiol. 1996; 31:696–708.
25. Petersein J, Saini S, Weissleder R. Liver. II: Iron oxide-based reticuloendothelial contrast agents for MR imaging. Clinical review. Magn. Reson. Imag. Clin. North Am. 1996; 4:53–60.
26. Weissleder R, Hahn PF, Stark DD, Elizondo G, Saini S, Todd LE, Wittenberg J, Ferrucci JT. Superparamagnetic iron oxide: enhanced detection of focal splenic tumors with MR imaging. Radiology. 1988; 169:399–403. [PubMed: 3174987]
27. Anzai Y, Blackwell KE, Hirschowitz SL, Rogers JW, Sato Y, Yuh WT, Runge VM, Morris MR, McLachlan SJ, Lufkin RB. Initial clinical experience with dextran-coated superparamagnetic iron oxide for detection of lymph node metastases in patients with head and neck cancer. Radiology. 1994; 192:709–715. [PubMed: 7520182]
28. Anzai Y, McLachlan S, Morris M, Saxton R, Lufkin RB. Dextran-coated superparamagnetic iron oxide, an MR contrast agent for assessing lymph nodes in the head and neck. Am. J. Neuroradiol. 1994; 15:87–94. [PubMed: 7511324]
29. Svenson S, Tomalia DA. Dendrimers in biomedical applications – reflections on the field. Adv. Drug Deliv. Rev. 2005; 57:2106–2129.
30. Tomalia DA, Reyna LA, Svenson S. Dendrimers as multi-purpose nanodevices for oncology drug delivery and diagnostic imaging. Biochem. Soc. Trans. 2007; 35:61–67. [PubMed: 17233602]
31. Kobayashi H, Brechbiel MW. Dendrimer-based macromolecular MRI contrast agents: characteristics and application. Mol. Imag. 2003; 2:1–10.
32. Cabanas RM. An approach for the treatment of penile carcinoma. Cancer. 1977; 39:456–466. [PubMed: 837331]
33. Krag D, Weaver D, Ashikaga T, Moffat F, Klimberg VS, Shriver C, Feldman S, Kusminsky R, Gadd M, Kuhn J, Harlow S, Beitsch P. The sentinel node in breast cancer – a multicenter validation study. N. Engl. J. Med. 1998; 339:941–946. [PubMed: 9753708]
34. Anzai Y. Superparamagnetic iron oxide nanoparticles: nodal metastases and beyond. Top. Magn. Reson. Imaging. 2004; 15:103–111. [PubMed: 15269613]
35. Guimaraes A, Tabatabei S, Dahl D, McDougal W, Weissleder R, Harisinghani M. Pilot study evaluating use of lymphotrophic nanoparticle-enhanced magnetic resonance imaging for assessing lymph nodes in renal cell cancer. Urology. 2008; 71:708–712. [PubMed: 18295316]
36. Harisinghani MG, Saksena M, Ross RW, Tabatabaei S, Dahl D, McDougal S, Weissleder R. A pilot study of lymphotrophic nanoparticle-enhanced magnetic resonance imaging technique in early stage testicular cancer: a new method for noninvasive lymph node evaluation. Urology. 2005; 66:1066–1071. [PubMed: 16286125]
37. Harisinghani MG, Barentsz J, Hahn PF, Deserno WM, Tabatabaei S, van de Kaa CH, de la Rosette J, Weissleder R. Noninvasive detection of clinically occult lymph-node metastases in prostate cancer. N. Engl. J. Med. 2003; 348:2491–2499. [PubMed: 12815134]
38. Kobayashi H, Kawamoto S, Star RA, Waldmann TA, Tagaya Y, Brechbiel MW. Micro-magnetic resonance lymphangiography in mice using a novel dendrimer-based magnetic resonance imaging contrast agent. Cancer Res. 2003; 63:271–276. [PubMed: 12543772]
39. Kobayashi H, Kawamoto S, Sakai Y, Choyke PL, Star RA, Brechbiel MW, Sato N, Tagaya Y, Morris JC, Waldmann TA. Lymphatic drainage imaging of breast cancer in mice by micro-magnetic resonance lymphangiography using a nano-size paramagnetic contrast agent. J. Natl. Cancer Inst. 2004; 96:703–708. [PubMed: 15126607]
40. Kobayashi H, Kawamoto S, Brechbiel MW, Bernardo M, Sato N, Waldmann TA, Tagaya Y, Choyke PL. Detection of lymph node involvement in hematologic malignancies using micromagnetic resonance lymphangiography with a gadolinum-labeled dendrimer nanoparticle. Neoplasia (New York). 2005; 7:984–991.
41. Reimer P, Jahnke N, Fiebich M, Schima W, Deckers F, Marx C, Holzknecht N, Saini S. Hepatic lesion detection and characterization: value of nonenhanced MR imaging, superparamagnetic iron

oxide-enhanced MR imaging, and spiral CT-ROC analysis. Radiology. 2000; 217:152–158. [PubMed: 11012438]

42. Kobayashi H, Kawamoto S, Saga T, Sato N, Hiraga A, Ishimori T, Akita Y, Mamede MH, Konishi J, Togashi K, Brechbiel MW. Novel liver macro-molecular MR contrast agent with a polypropylenimine diaminobutyl dendrimer core: comparison to the vascular MR contrast agent with the polyamidoamine dendrimer core. Magn. Reson. Med. 2001; 46:795–802. [PubMed: 11590657]
43. Vogl TJ, Kümmel S, Hammerstingl R, Schellenbeck M, Schumacher G, Balzer T, Schwarz W, Müller PK, Bechstein WO, Mack MG, Söllner O, Felix R. Liver tumors: comparison of MR imaging with Gd-EOB-DTPA and Gd-DTPA. Radiology. 1996; 200:59–67. [PubMed: 8657946]
44. Hosseinzadeh K, Schwarz SD. Endorectal diffusion-weighted imaging in prostate cancer to differentiate malignant and benign peripheral zone tissue. J. Magn. Reson. Imaging. 2004; 20:654–661. [PubMed: 15390142]
45. Guo Y, Cai YQ, Cai ZL, Gao YG, An NY, Ma L, Mahankali S, Gao JH. Differentiation of clinically benign and malignant breast lesions using diffusion-weighted imaging. J. Magn. Reson. Imaging. 2002; 16:172–178. [PubMed: 12203765]
46. Schmidt GP, Baur-Melnyk A, Herzog P, Schmid R, Tiling R, Schmidt M, Reiser MF, Schoenberg SO. High-resolution whole-body magnetic resonance image tumor staging with the use of parallel imaging versus dual-modality positron emission tomography-computed tomography: experience on a 32-channel system. Invest. Radiol. 2005; 40:743–753. [PubMed: 16304476]
47. Schlemmer H-P, Schäafer J, Pfannenberg C, Radny P, Korchidi S, Müller-Horvat C, Nägele T, Tomaschko K, Fenchel M, Claussen CD. Fast whole-body assessment of metastatic disease using a novel magnetic resonance imaging system: initial experiences. Invest. Radiol. 2005; 40:64–71. [PubMed: 15654249]
48. Krishnamurthy GT, Tubis M, Hiss J, Blahd WH. Distribution pattern of metastatic bone disease. A need for total body skeletal image. J. Am. Med. Assoc. 1977; 237:2504–2506.
49. Nakamoto Y, Osman M, Wahl RL. Prevalence and patterns of bone metastases detected with positron emission tomography using F-18 FDG. Clin. Nucl. Med. 2003; 28:302–307. [PubMed: 12642709]
50. Schmidt GP, Schoenberg SO, Schmid R, Stahl R, Tiling R, Becker CR, Reiser MF, Baur-Melnyk A. Screening for bone metastases: whole-body MRI using a 32-channel system versus dual-modality PET-CT. Eur. Radiol. 2007; 17:939–949. [PubMed: 16951929]
51. Engelhard K, Hollenbach HP, Wohlfart K, von Imhoff E, Fellner FA. Comparison of whole-body MRI with automatic moving table technique and bone scintigraphy for screening for bone metastases in patients with breast cancer. Eur. Radiol. 2004; 14:99–105. [PubMed: 12845463]
52. Steinborn MM, Heuck AF, Tiling R, Bruegel M, Gauger L, Reiser MF. Whole-body bone marrow MRI in patients with metastatic disease to the skeletal system. J. Comput. Assist. Tomogr. 1999; 23:123–129. [PubMed: 10050822]

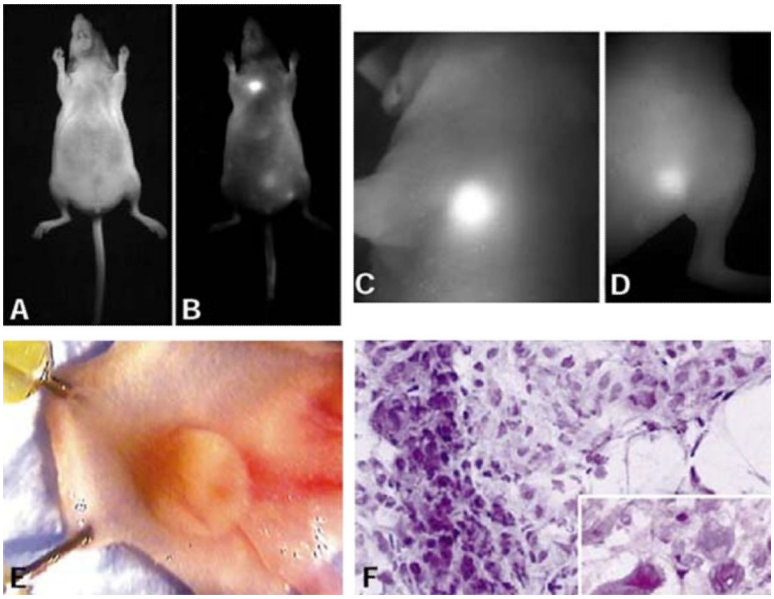

Figure 1.

LX-1 tumor implanted into the mammary fat pad of a nude mouse. (A) Light image. (B) Raw near-infrared (NIR) image. Note the bright tumor in the chest. (C) High-resolution NIR image of the chest wall tumor (2 mm). (D) High-resolution NIR image of the additional thigh tumor (< 0.3 mm). (E) Dissected tumor in the mammary pad. (F) Hematoxylin–eosin section of the NIR-positive tumor showing malignant and actively proliferating cells (magnification, × 200; inset, × 400). [These figures were reproduced from ref. (7) with permission obtained from *Nature Biotechnology*.]

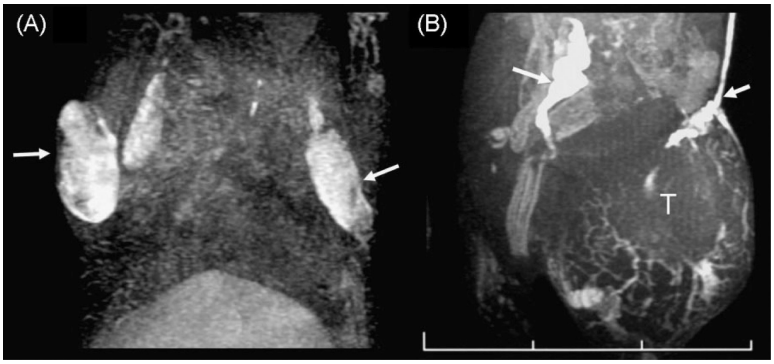

Figure 2.
Lymph node involvement of malignant lymphoma (A) and lymph node metastasis of colon cancer cells (B) visualized with the G6 dendrimer-based contrast agent in lymphangiographic MRI. Both lymph nodes are enlarged. The malignant lymphoma did not shut down the lymphatic flow, but made filling defects in the lymph nodes (A, arrows). In contrast, colon cancer metastasis (T) shut down the lymphatic flow and induced dilated collateral lymphatic vessels (B, arrows). One section of the scale bar indicates 1 cm.

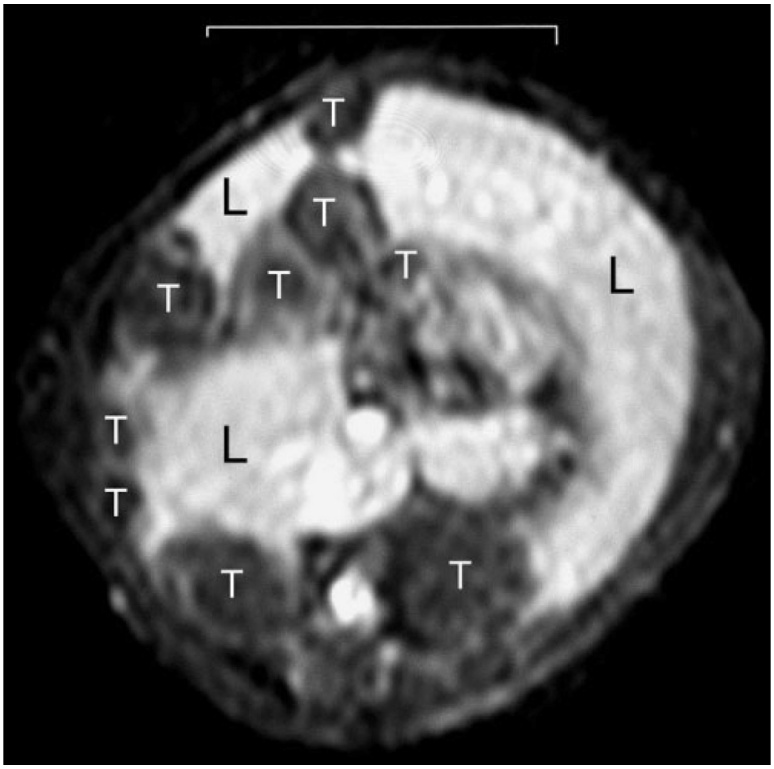

Figure 3.
Metastatic colon cancer tumors in the liver visualized with DAB-Am64-(1B4M-Gd)$_{64}$, a DAB/PPI-G5 dendrimer-based contrast agent. Liver parenchyma (L) is enhanced and tumors (T) are negatively depicted. The scale bar indicates 1 cm.

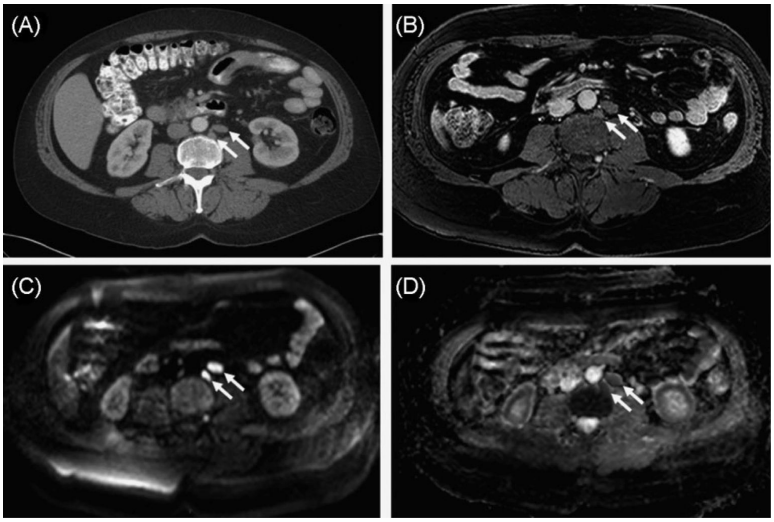

Figure 4.

Sixty-year-old man with prostate cancer. Axial contrast-enhanced computed tomography (A) and T_1-weighted MR (B) images demonstrate two slightly enlarged left retroperitoneal lymph nodes (arrows). Axial raw diffusion-weighted MR image (C) and apparent diffusion coefficient image (D) show increased (C) and decreased (D) signal intensity characteristics, consistent with restricted diffusion secondary to malignant infiltration of lymph nodes (arrows).